RSC Advances

ROYAL SOCIETY OF CHEMISTRY

www.rsc.org/advances

Segmental dynamics and physical aging of polystyrene/silver nanocomposites

Yu Lin,[ab] Langping Liu,[b] Jiaqi Cheng,[a] Yonggang Shangguan,[*a] Wenwen Yu,[a] Biwei Qiu,[a] and Qiang Zheng,[*a]

We report the complicated variation trend of calorimetric T_g and physical aging in PS/Ag nanocomposites, despite the invariant segmental dynamics with increasing silver nanoparticle loading.

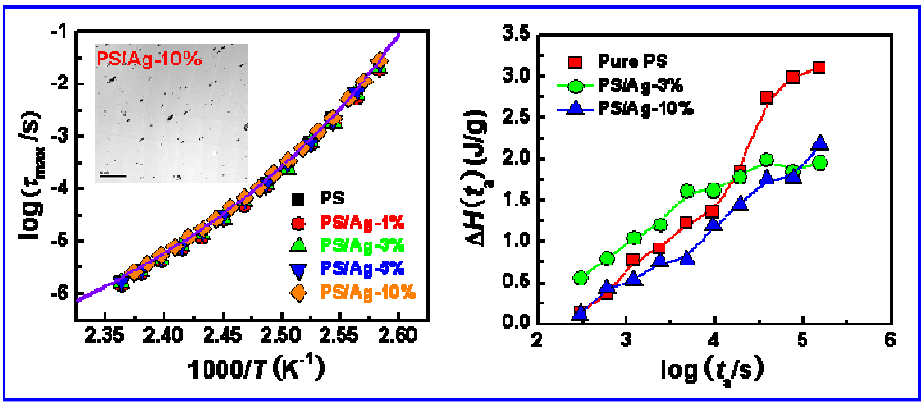

[*]Corresponding authors. Tel./fax: +86 571 8795 2522.
E-mail addresses: shangguan@zju.edu.cn (YG. Shangguan), zhengqiang@zju.edu.cn (Q. Zheng).

Segmental dynamics and physical aging of polystyrene/silver nanocomposites

Yu Lin,[ab] Langping Liu,[b] Jiaqi Cheng,[a] Yonggang Shangguan,[*a] Wenwen Yu,[a] Biwei Qiu,[a] and Qiang Zheng,[*a]

[a]*MOE Key Laboratory of Macromolecular Synthesis and Functionalization, Department of Polymer Science and Engineering, Zhejiang University, Hangzhou 310027, China*

[b]*Shanghai Key Laboratory of Advanced Polymeric Materials, School of Materials Science and Engineering, East China University of Science and Technology, Shanghai 200237, China*

Abstract: We investigate the effects of silver (Ag) nanoparticles on segmental and chain dynamics, physical aging and rheological behavior of polystyrene (PS) via a combination of broadband dielectric spectroscopy (BDS), calorimetry, and dynamic rheological measurement. The segmental dynamics of PS is found to be unchanged with increasing nanoparticle loading. After annealing below the glass transition temperature (T_g) for various time, by means of measuring the recovered enthalpy values of PS, it is surprising that an acceleration and a suppression of the physical aging in PS/Ag-3% and 10% nanocomposites can be observed, respectively, corresponding to the decreased and increased calorimetric T_g, which can be interpreted by plasticizing and antiplasticizing effects. Furthermore, the filler

[*]Corresponding authors. Tel./fax: +86 571 8795 2522.
E-mail addresses: shangguan@zju.edu.cn (YG. Shangguan), zhengqiang@zju.edu.cn (Q. Zheng).

reinforcement in rheological behavior is observed with increasing the weight fraction of Ag nanoparticles. The temperature-dependent horizontal shift factor reveals that the overall chain dynamics are shown to speed up in the presence of Ag nanoparticles. We also emphasize recent discrepancies in the literature works of polymer nanocomposites and polymer thin films by comparing our results.

Key words: Glass transition; Segmental dynamics; Chain dynamics; Physical aging

1. INTRODUCTION

Introduction of nanoparticles into polymers generate polymer nanocomposites (PNCs) with a combination of outstanding comprehensive properties, given by the integration of stiffness and stability of nanoparticles with the polymer excellent properties such as high transparency, mechanical, dielectric and processing properties, *etc*. More particularly, due to the unique electrical conductivity and antibacterial characteristics of silver (Ag) nanoparticles, polymer/Ag hybrid advanced materials have a vast array of applications in microelectronics devices, sensors and biomedical application. A fundamental understanding about polymer-nanoparticles interactions and dynamics will be of great significance to optimize structure and properties of such materials. Unfortunately, it has been poorly understood until now.[1, 2]

Glass transition temperature (T_g), which is directly related to the segmental dynamics, is one of the most fundamental parameters for amorphous polymers. In recent decades, the effects of nanoparticles on the T_g of PNCs have been extensively investigated. Due to the complexity of interactions including polymer-nanoparticle, polymer-polymer and nanoparticle-nanoparticle, a diverse range of effects could be

manifested. Green *et al*.[3] found that the T_gs of polymer-C_{60} mixtures increase and local polymer chain motions in the glassy state are suppressed compared with bulk polymers. Cabral *et al*.[4] and Ding *et al*.[5] also reported the similar deviations of T_g in other polymer-C_{60} nanocomposite systems. Schönhals *et al*.[6, 7] found that the T_g is by 30 K lower than that of pure polymers in polyethylene (PE) and polypropylene (PP) based layered double hydroxides (LDH) nanocomposites. Pandis *et al*.[8] also reveals that the glass transition becomes systematically faster in poly(methyl methacrylate) (PMMA)/Ag nanocomposites. Additionally, Green *et al*.[9] observed that PNCs may exhibit the increased or decreased T_g through controlling grafting density and chain length of nanoparticles. On the other hand, it has been reported that due to the reduced segmental mobility of bound layer in the vicinity of nanoparticles, PNCs containing different particles even exhibit two T_gs, corresponding to close bound and bulk chains.[10, 11] However, other investigations claimed no change in the segmental dynamics associated with T_g for PNCs.[12-15] Therefore, it is of great importance to interpret the essence of such discrepancies.

On the other hand, it is well known that amorphous polymers in the glass state are in a nonequilibrium state, and exist an excess of thermodynamic quantities such as volume or enthalpy. Note that physical aging refers to structure relaxation toward equilibrium, and it is generally accompanied by significant changes in physical properties such as mechanical strength, modulus and viscoelastic properties, *etc*.[16-18] The investigation of physical aging of PNCs will be of great significance because it is closely related to their long-term storage stability of PNCs materials. However,

similar to the above mentioned T_g results, the reported physical aging process of PNCs in previous literatures are also lack of consistency. Torkelson *et al*.[19-21] found that the physical aging is suppressed in the presence of nanoparticles. Many other studies also show the same reduction trends.[22-24] Nevertheless, Boucher *et al*.[25-27] demonstrated that the physical aging was shown to speed up in PMMA/silica and polystyrene (PS)/gold nanocomposites. Such controversies are generally attributed to the possible interactions between polymer and nanoparticles in PNCs.[27] However, as of now the mechanisms responsible for physical aging process in PNCs are not well understood.

In this study, the influences of Ag nanoparticles on the dynamics, physical aging and rheological behavior of PS are systematically investigated by means of broadband dielectric spectroscopy (BDS), calorimetry, and dynamic rheological measurement. The invariant segmental dynamics of PS in the presence of Ag nanoparticles was discussed through BDS isothermal frequency sweep. Whereas the suppression of physical aging and the rise of calorimetric T_g in the nanocomposites were studied by monitoring the recovered enthalpy by using DSC scans. Additionally, the filler reinforcement and the acceleration of overall chain dynamics in the nanocomposites were probed by rheological measurement.

2. EXPERIMENTAL SECTION

2.1 Materials and sample preparation

Polystyrene (PS, M_w = 140 kg/mol, M_w/M_n = 2.1) was purchased from Sigma-Aldrich. Ag nanoparticles with an average particle size of 50 nm were obtained

from Beijing DK Nano technology Co. Ltd., China. All materials were used as received. Solution mixing and rapid precipitation described elsewhere[2, 4] were employed to prepare well dispersed PS/Ag nanocomposites in this study. Ag nanoparticles were dispersed in tetrahydrofuran (THF) and ultrasonicated for 30 min in a water bath. Then the PS was dissolved in the THF solution at 3% by weight with continuous stirring for 2 h, and bath-sonicated again for 30 min. Finally, the solution was then precipitated in 500 mL methanol, washed with deionized water and filtrated. The samples were kept at room temperature for 24 h, and then transferred to a vacuum oven at 403 K (well above the T_g of PS) for at least 72 h to remove residual solvent. Thermogravimetry analysis (TGA) was performed to verify the nanoparticle weight fraction and the complete evaporation of solvent. PS/Ag nanocomposites at various nanoparticle concentrations (1, 3, 5, 10 wt%) were prepared by using this method. The samples were compression-molded at 10 Mpa and 160 ^{o}C into approximate 100 μm thickness films and disc samples with a diameter of 25 mm and a thickness of 1.5 mm for dielectric and rheological measurements, respectively.

2.2 Characterization of the nanocomposites

Transmission electron microscope (TEM, JEM-1230, JEOL, Japan) at an acceleration voltage of 100 kV was employed to observe the nanoparticle dispersion morphology in the nanocomposites. Nanocomposite ultra-thin sections of about 100 nm in thickness were microtomed at room temperature from the prepared disc samples.

Broadband dielectric spectroscopy (BDS) measurements were conducted on a

Novocontrol Alpha high-resolution dielectric analyzer (Novocontrol GmbH Concept 40, Novocontrol Technology, Germany), and the temperature was controlled by a Novocool cryogenic system with a precision of ±0.1 K during the experiments. The films of 100 μm in thickness were placed between two parallel gold electrodes of 20 mm diameter. Isothermal frequency sweeps recording the dielectric function every 3 K were carried out over the temperature range from 363 to 433 K in the frequency range of 10^{-1} ~ 10^{7} Hz. Temperature sweeps were performed from 273 to 433 K at the frequency of 10 Hz and the heating rate of 3 K/min.

Differential scanning calorimetry (DSC) measurements were performed on a differential scanning calorimeter (Q100, TA, USA) to detect the T_g and physical aging of PS/Ag nanocomposites. Pure indium was employed for temperature calibration. All the measurements were carried out under a nitrogen atmosphere. For the T_g measurement, the samples were first heated to 423 K and kept for 5 min to eliminate thermal history, and then cooled down to 313 K to obtain the T_g determined by the TA Universal Analysis 2000 software. For the measurement of physical aging, all the samples were first heated to 423 K and kept for 5 min to eliminate thermal history, and subsequently cooled down to 313 K at the rate of 20 K/min. Afterward, the samples were aged in the DSC at the aging temperature (T_a) kept for enthalpy relaxation at various aging time (t_a) from 5 to 320 min, prior to being cooled down to 313 K at the cooling rate of 20 K/min, and finally they were reheated to 423 K at 10 K/min for data collection. For longer time physical aging measurements, the annealing of the samples was carried out in a vacuum oven at T_a for various aging

time (from 640 to 2560 min), after erasing the thermal history and quenching of the samples in the DSC. The samples were quenched again after aging and DSC thermograms were recorded for data collection.

The rheological measurements were carried out on an advance rheometric expansion system (ARES-G2, TA, USA) with parallel plate geometry of 25 mm in diameter. Isothermal frequency sweeps recording the viscoelastic properties every 10 K were applied in the frequency range of 10^{-2} ~ 10^{2} rad/s from 433 to 473 K. The strain amplitude was 1%, ensuring that all the measurements were in the linear viscoelastic region.

3. RESULTS AND DISCUSSION

3.1 Characterization of PS/Ag nanocomposites

Fig. 1 illustrates the quality of Ag dispersion in PS/Ag nanocomposites at the weight fraction of 3% and 10%. From Fig. 1 one can estimate that the Ag nanoparticles show an average diameter 50 nm, consistent with the quantitative measurement results using the TEM images and Nano Measurer software, as shown in Fig. S1. It can be found that the average diameter of Ag nanoparticles is 52.1 nm with a relative wide polydispersity according to a large quantity of statistics results. Generally, the dispersion is reasonably homogeneous across the observed sample area, despite that a visible aggregation of Ag nanoparticles could be detectable in the PNCs samples. This indicates that even after sonication treatment the aggregates of nanoparticles could be notable, though solution mixing and rapid precipitation method worked well. On the other hand, high temperature (403 K) drying process for long

time (72 h) during sample preparation could induce the formation of aggregates, as described in other PNCs system upon annealing.[28] Sangoro *et al*.[2] and Boucher *et al*.[27] also reported the formation of aggregates in poly(2-vinylpyridine) (P2VP)/oxide nanoparticles and PS/gold nanocomposites, and they investigated that the aggregation of the nanoparticles do not play a great role in the molecular dynamics and physical aging of nanocomposites provided the overall well dispersion.

3.2 Segmental dynamics of PS/Ag nanocomposites

Firstly, we investigate the effect of Ag nanoparticles on the segmental dynamics of PS. Fig. 2 shows the temperature dependences of dielectric loss ε'' for different PS/Ag nanocomposites. It is noted that the temperature and main relaxation time corresponding to the maximum of dielectric loss (ε''_{max}) is substantially equal for pure PS and its nanocomposites, indicating that the segmental dynamics of PS is not obviously altered by introduction of Ag nanoparticles into PS matrix. It is similar to the results of PS/gold nanocomposites reported by Boucher *et al*.[27] Moreover, Fig. 2 shows that the width of the dielectric loss function is not noticeably changed by the addition of Ag nanoparticles, in agreement with PMMA/silica nanocomposites,[26] which can be attributed to the unchanged heterogeneous dynamics. This differs from the significant broadening of dielectric spectra found in PS/gold nanocomposites.[27] It is expected that a broader spectral shape of segmental relaxation can be exhibited due to the increasing heterogeneities in the presence of nanoparticles.[15, 29] However, neither the main relaxation time nor the width of the spectra is affected by nanoparticle loading in PS/Ag nanocomposites presented here. The detailed analysis

of the shape parameters are also discussed in detail in the following.

To further quantitatively study the effect of Ag nanoparticle on the segmental dynamics of PS, the detailed analysis of relaxation time should be revealed. Fig. 3 shows the frequency dependences of dielectric loss ε'' for pure PS. At the temperature range investigated, one relaxation peak identified as α-relaxation can be observed, which is associated with the segmental motion of PS. The similar trend of PS/Ag nanocomposite results can be found in Fig. S2. In the literature reported previously,[27, 29-31] a weak second relaxation process (β^*) of PS displays in the high frequency region, though the mechanism is still ambiguous. Nevertheless, the β^*-process is not clearly noted in our study.

In order to extract quantitative information from the isothermal dielectric measurements, the complex dielectric function was analyzed by using the empirical Havriliak-Negami (HN) function.[32]

$$\varepsilon^* = \varepsilon_\infty + \frac{\Delta\varepsilon}{\left[1+\left(i\omega\tau_{\mathrm{HN}}\right)^{\alpha_{\mathrm{HN}}}\right]^{\beta_{\mathrm{HN}}}} - i\frac{\sigma}{\varepsilon_0\omega^s} \quad (1)$$

in which, ω is angular frequency ($\omega = 2\pi f$), $\Delta\varepsilon$ is the dielectric strength, ε_∞ is the unrelaxed value of the dielectric constant, τ_{HN} is the HN relaxation time, and the exponents α_{HN} and β_{HN} are shape parameters describing the symmetric and asymmetric broadening of the spectra, respectively. An additional conductivity effect was taken into account by adding a contribution $-i(\sigma/(\varepsilon_0\omega^s))$ to Eq. 1, where σ is the dc conductivity constant, ε_0 is the dielectric permittivity of vacuum, and the coefficient s characterizes the conduction mechanism. As shown in Fig. 3, the HN function including a conductivity process was used to fit the isothermal dielectric

spectra in this study. Furthermore, the HN relaxation time τ_{HN} is related to the mean molecular relaxation time τ_{max} corresponding to the maximum of the dielectric loss by the equation

$$\tau_{max} = \tau_{HN}\left(\sin\frac{\alpha_{HN}\beta_{HN}\pi}{2(\beta_{HN}+1)}\right)^{1/\alpha_{HN}}\left(\sin\frac{\alpha_{HN}\pi}{2(\beta_{HN}+1)}\right)^{-1/\alpha_{HN}} \quad (2)$$

Fig. 4 shows the temperature dependences of segmental relaxation time for PS and its nanocomposites. The introduction of Ag nanoparticle has no significant effect on the segmental dynamics of PS even at high loadings (10%). The results are in agreement with that of PS/Ag nanocomposites and invariant segmental dynamics in PS thin films with decreasing the thickness.[27, 33] This is also consistent with the finding in many other PNCs reported previously.[2, 12-15, 25, 26, 34] Nevertheless, a suppression of segmental dynamics of PNCs has been reported in the literature due to the reduced mobility resulting from strong attractive interactions between polymer and nanoparticle.[5, 35, 36] Even in the absence of specific polymer-filler interactions, natural rubber/silica nanocomposites show restricted segmental mobility compared to bulk polymer.[37] However, many other studies reveal that the segmental dynamics become systematically faster in the presence of nanoparticles due to various nanoparticle radius and feature, and interactions between polymer and nanoparticle.[6, 7, 38] In contrast with our result presented here, Cabral *et al*.[4] and Schönhals *et al*.[29] demonstrated that the segmental motion was shown to speed up in PS/C_{60} and PS/Phenethyl-POSS nanocomposites. In the same way, the accelerated segmental dynamics of PMMA/Ag nanocomposites are obtained due to the small size of Ag nanoparticles (5.6 nm).[8] Additionally, Green *et al*.[9] investigated the dynamics of

PS/gold nanocomposites and proved that the gold nanoparticle may exhibit plasticization or antiplasticization effects through controlling the grafting density and chain length of gold nanoparticles. Such difference between our result and the above mentioned literatures could be mainly ascribed to the absence of strong polymer-nanoparticle interactions because the Ag nanoparticle is not treated by grafting polymerization or surface treatment in this study, as indicated by the FTIR spectra results shown in Fig. S3. Looking at the spectra of pure PS and its nanocomposites, the identical peaks can be observed and no shift or new absorption band can be observed. The other important reason can be attributed to the fact that the average particle size (52.1 nm) is much larger herein, while the size of particles are very small (several nanometers) and can be compared with the radius of gyration of the polymer chains in the literatures.[4, 8, 9]

Furthermore, the temperature dependences of α-relaxation time can be described by the Vogel-Fulcher-Tamman (VFT) equation

$$\log \tau_{\max} = \log \tau_0 + \frac{A}{T - T_0} \tag{3}$$

where τ_0 is the infinite relaxation time, A is related to the fragility of the system, and T_0 is the Vogel temperature. As shown in Fig. 4, the fits can be well described by the same fitting parameters for all samples. And the values of τ_0, A, and T_0 is $10^{-11.5}$ s, 505.4 K and 336.5 K, respectively, further indicating the invariant segmental dynamics by Ag nanoparticle loading. On the other hand, Fig. S4 represents the shape parameters of the α-relaxation at 393 K for PS/Ag nanocomposites with various Ag nanoparticle concentrations. It can be seen that the α_{HN} and β_{HN} values are almost

unchanged with increasing Ag nanoparticle loading, indicating that the width and symmetry of the α-relaxation spectra are hardly affected, which is consistent with the temperature sweep results shown in Fig. 2. Hence, we can conclude that neither the dynamics nor the distribution width of the segmental motion in PS/Ag nanocomposites is affected by the Ag nanopartilces.

3.3 Physical aging of PS/Ag nanocomposites

In this section, we further investigate the physical aging of PS and PS/Ag nanocomposites by monitoring their enthalpy relaxation by using DSC. In order to ensure that the segmental mobility is identical for all samples, the physical aging has been studied at the same aging temperature due to the fact that the segmental dynamics is not altered by Ag nanoparticle loading as discussed above. Fig. 5 shows the typical thermograms obtained from DSC for PS and its nanocomposites after physical aging at 363 K for various aging time. From the DSC traces in Fig. 5, it is obvious that the enthalpy relaxation peaks appear and the intensity increases with increasing aging time. Moreover, longer annealing time should be needed in oder to achieve the plateau value of recovered enthalpy.

Furthermore, the amount of recovered enthalpy of amorphous polymers annealed at a given aging temperature T_a for various time t_a can be calculated by integration of the difference between the measured heat capacity of the aged and unaged samples, expressed as:[27, 39]

$$\Delta H\left(T_a, t_a\right) = \int_{T_1}^{T_2} \left(C_P^a\left(T\right) - C_P^u\left(T\right)\right) dT \quad (4)$$

in which, $C_P^a\left(T\right)$ and $C_P^u\left(T\right)$ are the heat capacity of the aged and unaged samples,

respectively. T_1 and T_2 represent the reference temperatures ($T_1 < T_g < T_2$).

In order to quantitatively analyze the effect of Ag nanoparticle on the enthalpy relaxation of PS, a comparison of recovered enthalpy $\Delta H(t_a)$ as a function of aging time for PS and its nanocomposites is shown in Fig. 6. Surprisingly, totally different physical aging behavior can be observed for PS/Ag-3% and 10% nanocomposites, respectively. For PS/Ag-3% nanocomposites, it can be noted that the values of $\Delta H(t_a)$ are higher than that of pure PS, suggesting an acceleration of physical aging. These findings agree well with the results of PMMA/silica and PS/gold nanocomposites reported by Boucher *et al*.,[25-27] and polymer thin or ultrathin films.[40-42] However, the physical aging is shown to slow down in PS/Ag-10% nanocomposites. The suppression of physical aging appears to be consistent with the tendency observed in the literature works dealing with other types of polymer nanocomposite systems.[19-24] From Fig. 6, we can also observed that the equilibrium values of $\Delta H(t_a)$ can be achieved in a shorter time for PS/Ag-3% nanocomposites compared with pure PS, while the situation is just the opposite for PS/Ag-10% nanocomposites, which further verifing the acceleration and suppression of physical aging above mentioned.

It is generally accepted that a model based on diffusion of free volume holes toward the polymer-nanoparticle interfaces can be used to quantitatively describe the physical aging and calorimetric T_g in PNCs samples.[25-27] Hence, the calorimetric T_g defined as the mid-point of glass transition from DSC curve is investigated, as shown Fig. 7. For PS/Ag-3% samples, the value of T_g is 376.5 K, which is lower than that of pure PS (377.6 K). The results agree well with the decrease tendency in T_g observed in other

studies dealing with PNCs system,[6-8, 25-27] polymer thin or ultrathin films.[40-42] But the increased calorimetric T_g can be detected in PS/Ag-10% nanocomposites. Such discrepancies in previous works are mainly due to different preparation methods (residual solvent, annealing time, thermal history, *etc*.) or various experimental conditions (measurement apparatus, atmosphere, rate, ambient humidity, *etc*.).[43, 44] These factors can be ignored in this study because all of the experimental conditions are uniform. The difference between PS/Ag-3% and 10% can be interpreted as follows: For PS/Ag nanocomposites with low Ag nanoparticle loading, the plasticization of the PS matrix plays a dominant role due to constraints imposed to packing of the chains by the Ag nanoparticles, and, at the same time, the absence of strong polymer-nanoparticle interactions because Ag nanoparticles are not treated by surface modification in this study, which is consistent with the finding reported by Pandis *et al*.[8] However, for PS/Ag nanocomposites with high concentration of Ag nanoparticle, the antiplasticization effects can be observed due to an increase of the fragility of glass formation and the increased chain barrier between nanoparticles. Therefore, the calorimetric T_g increases and physical aging is shown to slow down with further increasing Ag nanoparticle loading.

On the other hand, the variation trend of T_g is seemingly anomalous compared with the invariant segmental dynamics discussed above. It is worthy noted that the T_g of amorphous polymers probed by DSC corresponds to its transition from equilibrium liquid-like to non-equilibrium glassy state,[27, 45] whereas BDS tests measure the segmental dynamics at equilibrium. Boucher *et al*.[25-27, 33] reported the T_g depression

and invariant segmental dynamics in PS thin films, PMMA/silica and PS/gold nanocomposites. In contrast, we observe the decreased and increased T_g, and unchanged segmental dynamics in this study. Based on these observations mentioned above, we can conclude that the variation trend of calorimetric T_g and physical aging in PS/Ag nanocomposites further verify the fact that the physical aging is driven by the diffusion toward the polymer-nanoparticle interfaces.[25-27]

3.4 Rheological behavior of PS/Ag nanocomposites

As discussed above, the invariant segmental dynamics by Ag nanoparticle loading can be observed. Furthermore, the dynamic rheological measurement has been carried out in order to investigate the dynamics on a larger scale (chain dynamics) of PS with increasing Ag nanoparticle loading. Fig. 8 shows the linear viscoelastic properties of pure PS and PS/Ag nanocomposites during isothermal frequency sweep at 473 K. It can be observed that the dynamic storage modulus (G'), loss modulus (G'') and complex viscosity (η^*) increases with increasing the Ag nanoparticle loading, indicating that common filler reinforcement takes place. The same tendency appears at other temperatures. Additionally, the influences of Ag nanoparticle on the chain dynamics of PS can be well discussed using time-temperature superposition (TTS) curves of rheological measurements. Fig. 9 shows the master curves for G' and G'' of pure PS and PS/Ag nanocomposites. One can see that the TTS principle constructed by using the horizontal shift factor α_T holds well for both neat PS and its nanocomposites. However, a suppression of the terminal behavior at low frequencies is not observed, indicating the absence of the formation of large-scale nanoparticle

network, as shown in Fig. 1. These observations appear to be in disagreement with works finding a second plateau in the terminal region of PNCs with high nanoparticle loading due to the formation of particle network.[2, 46, 47] Furthermore, the temperature dependences of horizontal shift factor α_T is analyzed in detail, as shown in Fig. 10. It can be found that the value of α_T increases with increasing the weight percentage of Ag nanoparticle, implying that the overall chain dynamics is shown to speed up in PS/Ag nanocomposites, though Ag nanoparticles do not significantly influence the segmental dynamics and terminal rheological behaviors at low frequencies. However, Sangoro *et al*.[2] reported that neither the segmental dynamics nor the chain dynamics is altered by the oxide nanoparticles in P2VP/TiO_2 nanocomposites. These observed differences mainly result from different interactions, preparation methods or experimental conditions.[43, 44] The faster chain dynamics can be attributed to the fact that the packing of the PS chains are constrained by Ag nanoparticles due to the absence of strong polymer-nanoparticle interactions.[8]

4. SUMMARY

The influences of Ag nanoparticles on segmental dynamics, physical aging and rheological behaviors were investigated by using BDS, calorimetry and rheology. The BDS measurements reveal that the segmental dynamics of PS is not altered in the presence of Ag nanoparticles. However, totally different physical aging behavior can be observed for PS/Ag-3% and 10% nanocomposites. It can be seen that the calorimetric T_g decreases and physical aging shows to speed up in PS/Ag-3% nanocomposites, whereas the increased calorimetric T_g and a suppresion of physical

aging can be noted. These results can be attributed to plasticizing and antiplasticizing effects for nanocomposites with low and high nanoparticle loading, respectively. Moreover, filler reinforcement takes place with increasing Ag nanoparticle loading by using rheological measurements. We also report an acceleration of overall chain dynamics due to the constrained chain packing by the Ag nanoparticles, despite the invariant segmental dynamics and terminal rheological behavior.

ACKNOWLEDGEMENTS

This work was supported by the National Nature Science Foundation of China (No. 51173165) and the Fundamental Research Funds for the Central Universities (No. 2013QNA4048).

REFERENCES

1 C. G. Robertson and C. M. Roland, *Rubber Chem. Technol.*, 2008, **81**, 506-522.

2 A. P. Holt, J. R. Sangoro, Y. Y. Wang, A. L. Agapov and A. P. Sokolov, *Macromolecules*, 2013, **46**, 4168-4173.

3 J. M. Kropka, V. G. Sakai and P. F. Green, *Nano Lett.*, 2008, **8**, 1061-1065.

4 H. C. Wong, A. Sanz, J. F. Douglas and J. T. Cabral, *J. Mol. Liq.*, 2010, **153**, 79-87.

5 Y. F. Ding, S. Pawlus, A. P. Sokolov, J. F. Douglas, A. Karim and C. L. Soles, *Macromolecules*, 2009, **42**, 3201-3206.

6 A. Schoenhals, H. Goering, F. R. Costa, U. Wagenknecht and G. Heinrich, *Macromolecules*, 2009, **42**, 4165-4174.

7 P. J. Purohit, J. E. Huacuja-Sanchez, D. Y. Wang, F. Emmerling, A. Thunemann, G. Heinrich and A. Schonhals, *Macromolecules*, 2011, **44**, 4342-4354.

8 C. Pandis, E. Logakis, A. Kyritsis, P. Pissis, V. V. Vodnik, E. Dzunuzovic, J. M. Nedeljkovic, V. Djokovic, J. C. R. Hernandez and J. L. G. Ribelles, *Eur. Polym. J.*, 2011, **47**, 1514-1525.

9 H. Oh and P. F. Green, *Nat. Mater.*, 2009, **8**, 139-143.

10 G. Tsagaropoulos and A. Eisenburg, *Macromolecules*, 1995, **28**, 396-398.

11 L. Chen, K. Zheng, X. Y. Tian, K. Hu, R. X. Wang, C. Liu, Y. Li and P. Cui, *Macromolecules*, 2010, **43**, 1076-1082.

12 R. B. Bogoslovov, C. M. Roland, A. R. Ellis, A. M. Randall and C. G. Robertson, *Macromolecules*, 2008, **41**, 1289-1296.

13 M. Hernandez, J. Carretero-Gonzalez, R. Verdejo, T. A. Ezquerra and M. A. Lopez-Manchado, *Macromolecules*, 2010, **43**, 643-651.

14 J. Otegui, G. A. Schwartz, S. Cerveny, J. Colmenero, J. Loichen and S. Westermann, *Macromolecules*, 2013, **46**, 2407-2416.

15 J. Mijovic, H. K. Lee, J. Kenny and J. Mays, *Macromolecules*, 2006, **39**, 2172-2182.

16 I. M. Hodge, *Science*, 1995, **267**, 1945-1947.

17 J. M. Hutchinson, *Prog. Polym. Sci.*, 1995, **20**, 703-760.

18 C. H. Ahn, W. H. Jo and M. S. Lee, *Polym. J.*, 2000, **32**, 471-475.

19 R. D. Priestley, C. J. Ellison, L. J. Broadbelt and J. M. Torkelson, *Science*, 2005, **309**, 456-459.

20 P. Rittigstein, R. D. Priestley, L. J. Broadbelt and J. M. Torkelson, *Nat. Mater.*, 2007, **6**, 278-282.

21 R. D. Priestley, P. Rittigstein, L. J. Broadbelt, K. Fukao and J. M. Torkelson, *J. Phys.: Condens. Matter*, 2007, **19**, 205120-205132.

22 H. B. Lu and S. Nutt, *Macromol. Chem. Phys.*, 2003, **204**, 1832-1841.

23 S. Amanuel, A. N. Gaudette and S. S. Sternstein, *J. Polym. Sci., Part B: Polym. Phys.*, 2008, **46**, 2733-2740.

24 A. L. Flory, T. Ramanathan and L. C. Brinson, *Macromolecules*, 2010, **43**, 4247-4252.

25 V. M. Boucher, D. Cangialosi, A. Alegria and J. Colmenero, *Macromolecules*, 2010, **43**, 7594-7603.

26 V. M. Boucher, D. Cangialosi, A. Alegria, J. Colmenero, J. Gonzalez-Irun and L. M. Liz-Marzan, *Soft Matter*, 2010, **6**, 3306-3317.

27 V. M. Boucher, D. Cangialosi, A. Alegria, J. Colmenero, I. Pastoriza-Santos and L. M. Liz-Marzan, *Soft Matter*, 2011, **7**, 3607-3620.

28 Y. Q. Tan, X. Z. Yin, M. T. Chen, Y. H. Song and Q. Zheng, *J. Rheol.*, 2011, **55**, 965-979.

29 N. Hao, M. Boehning and A. Schoenhals, *Macromolecules*, 2007, **40**, 9672-9679.

30 C. Svanberg, *Macromolecules*, 2007, **40**, 312-315.

31 V. Lupascu, S. J. Picken and M. Wubbenhorst, *Macromolecules*, 2006, **39**, 5152-5158.

32 S. Havriliak and S. Negami, *Polymer*, 1967, **8**, 161-210.

33 V. M. Boucher, D. Cangialosi, H. J. Yin, A. Schonhals, A. Alegria and J. Colmenero, *Soft Matter*, 2012, **8**, 5119-5122.

34 M. Hernandez, M. D. Bernal, R. Verdejo, T. A. Ezquerra and M. A. Lopez-Manchado, *Compos. Sci. Technol.*, 2012, **73**, 40-46.

35 M. Hernandez, T. A. Ezquerra, R. Verdejo and M. A. Lopez-Manchado, *Macromolecules*, 2012, **45**, 1070-1075.

36 L. T. Vo, S. H. Anastasiadis and E. P. Giannelis, *Macromolecules*, 2011, **44**, 6162-6171.

37 D. Fragiadakis, L. Bokobza and P. Pissis, *Polymer*, 2011, **52**, 3175-3182.

38 N. Hao, M. Bohning, H. Goering and A. Schonhals, *Macromolecules*, 2007, **40**, 2955-2964.

39 I. Hodge, *J. Non-Cryst. Solids*, 1994, **169**, 211-266.

40 K. D. Dorkenoo and P. H. Pfromm, *Macromolecules*, 2000, **33**, 3747-3751.

41 Y. P. Koh, G. B. McKenna and S. L. Simon, *J. Polym. Sci., Part B: Polym. Phys.*, 2006, **44**, 3518-3527.

42 Y. P. Koh and S. L. Simon, *J. Polym. Sci., Part B: Polym. Phys.*, 2008, **46**, 2741-2753.

43 M. Erber, M. Tress, E. U. Mapesa, A. Serghei, K. J. Eichhorn, B. Voit and F. Kremer, *Macromolecules*, 2010, **43**, 7729-7733.

44 H. K. Nguyen, M. Labardi, S. Capaccioli, M. Lucchesi, P. Rolla and D. Prevosto, *Macromolecules*, 2012, **45**, 2138-2144.

45 J. A. Forrest and K. Dalnoki-Veress, *Adv. Colloid Interface Sci.*, 2001, **94**, 167-196.

46 Q. Zheng, B. B. Yang, G. Wu and L. W. Li, *Chem. J. Chin. Univ.-Chin.*, 1999, **20**, 1483-1490.

47 G. Filippone and M. S. de Luna, *Macromolecules*, 2012, **45**, 8853-8860.

Figure captions

Fig. 1 TEM images of nanoparticle distributions in (a) PS/Ag-3% and (b) PS/Ag-10% nanocomposites.

Fig. 2 Temperature dependences of dielectric loss at a frequency of 10 Hz for pure PS and PS/Ag nanocomposties.

Fig. 3 Dielectric loss as a function of frequency for pure PS at various temperatures. The solid lines are fits to the data using the HN function including the conductivity and interfacial process contributions. The dash dot lines represent the α-relaxation process. The dashed lines are the contribution of the conductivity.

Fig. 4 Segmental relaxation time as a function of temperature for pure PS and PS/Ag nanocomposties. The solid curve represents VFT fit to the data.

Fig. 5 DSC heating curves of (a) pure PS, (b) PS/Ag-3% and (c) PS/Ag-10% nanocomposites after physical aging at 363 K for various aging time.

Fig. 6 Aging time dependences of recovered enthalpy $\Delta H(t_a)$ for pure PS and PS/Ag nanocomposites at the aging temperature of 363 K.

Fig. 7 DSC curves of pure PS and its nanocomposites at the cooling rate of 10 K/min. The solid lines show the position of T_g.

Fig. 8 Frequency dependences of (a) dynamic storage modulus (open symbols) and loss modulus (filled symbols) and (b) complex viscosity for pure PS and PS/Ag nanocomposites at 473 K.

Fig. 9 Master curves of dynamic storage modulus (open symbols) and loss modulus

(filled symbols) for (a) pure PS, (b) PS/Ag-3% and (c) PS/Ag-10% nanocomposites at the reference temperature of 433 K. (□, ■) 433 K, (○, ●) 443 K, (△, ▲) 453 K, (▽, ▼) 463 K and (◇, ◆) 473 K.

Fig. 10 Temperature dependences of horizontal shift factors for pure PS and PS/Ag nanocomposites at the reference temperature of 433 K.

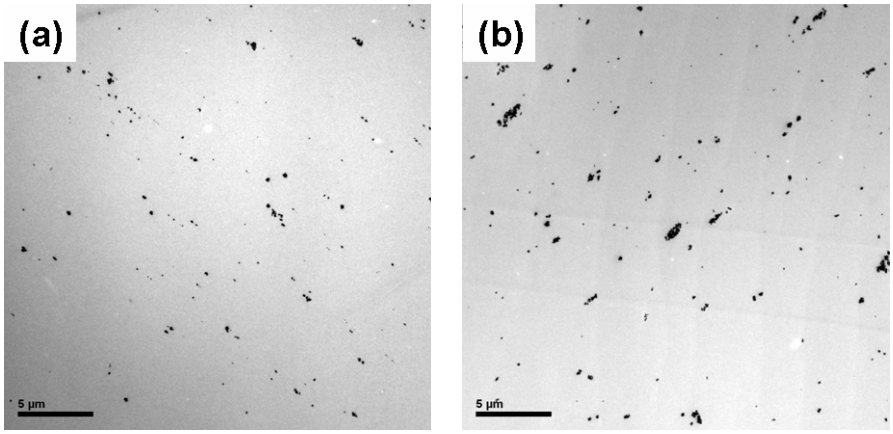

Fig. 1 TEM images of nanoparticle distributions in (a) PS/Ag-3% and (b) PS/Ag-10% nanocomposites.

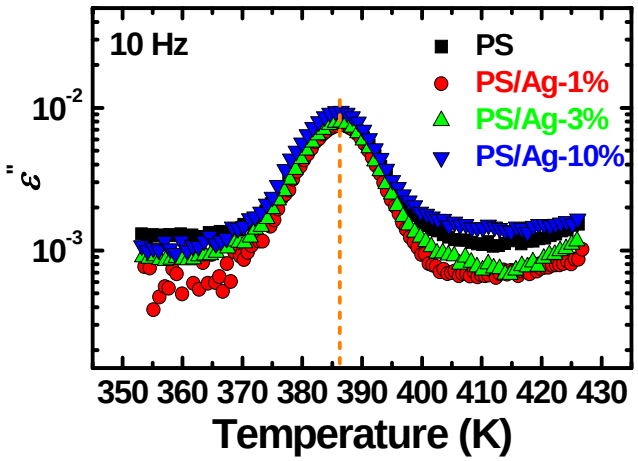

Fig. 2 Temperature dependences of dielectric loss at a frequency of 10 Hz for pure PS and PS/Ag nanocomposties.

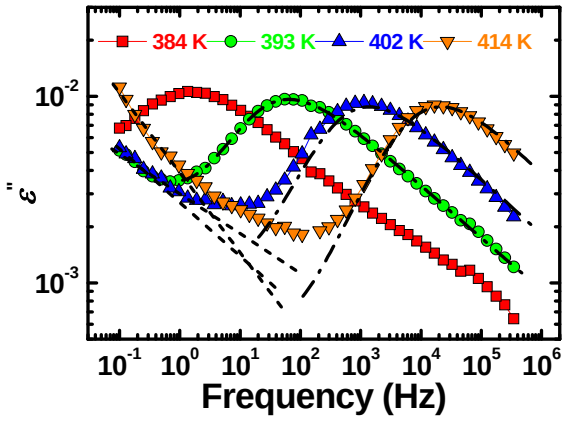

Fig. 3 Dielectric loss as a function of frequency for pure PS at various temperatures. The solid lines are fits to the data using the HN function including the conductivity and interfacial process contributions. The dash dot lines represent the α-relaxation process. The dashed lines are the contribution of the conductivity.

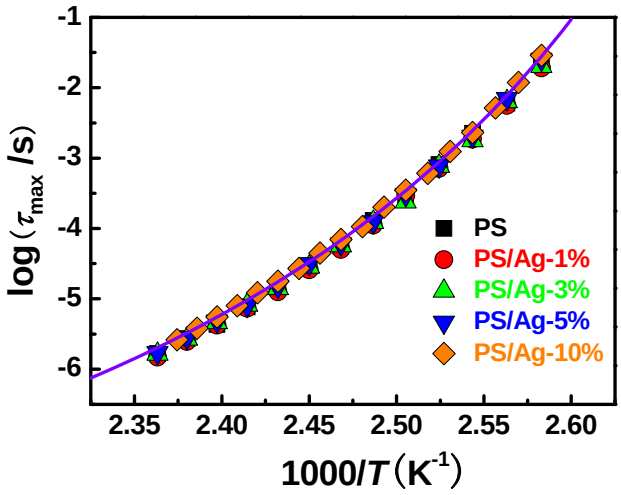

Fig. 4 Segmental relaxation time as a function of temperature for pure PS and PS/Ag nanocomposties. The solid curve represents VFT fit to the data.

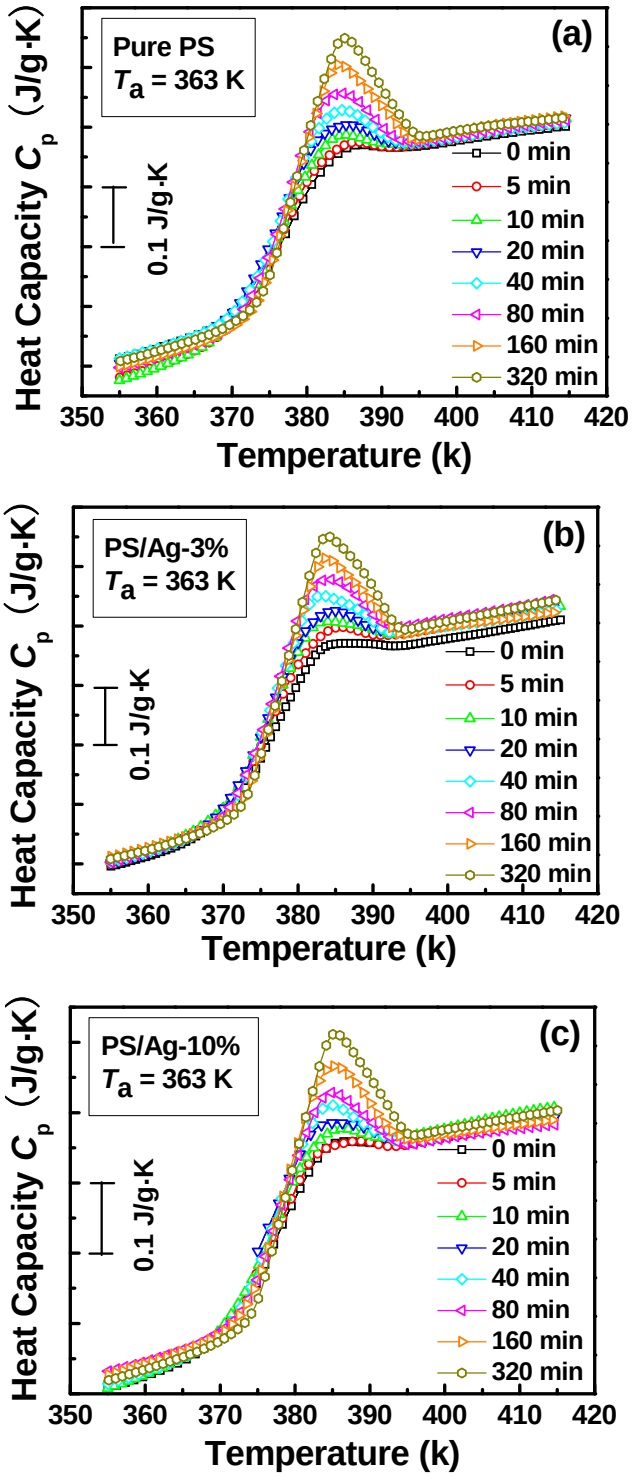

Fig. 5 DSC heating curves of (a) pure PS, (b) PS/Ag-3% and (c) PS/Ag-10% nanocomposites after physical aging at 363 K for various aging time.

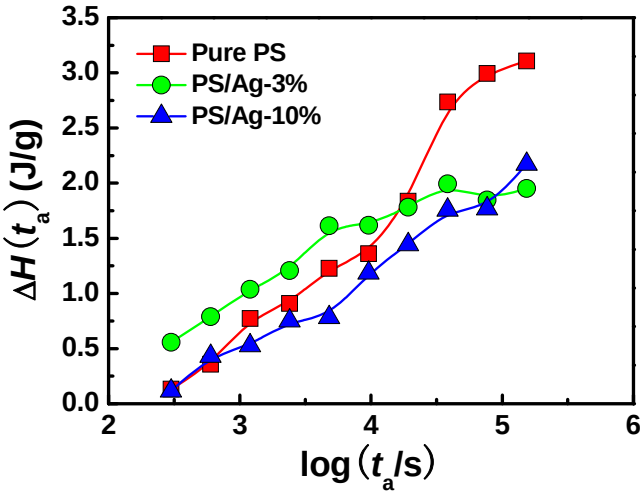

Fig. 6 Aging time dependences of recovered enthalpy $\Delta H(t_a)$ for pure PS and PS/Ag nanocomposites at the aging temperature of 363 K.

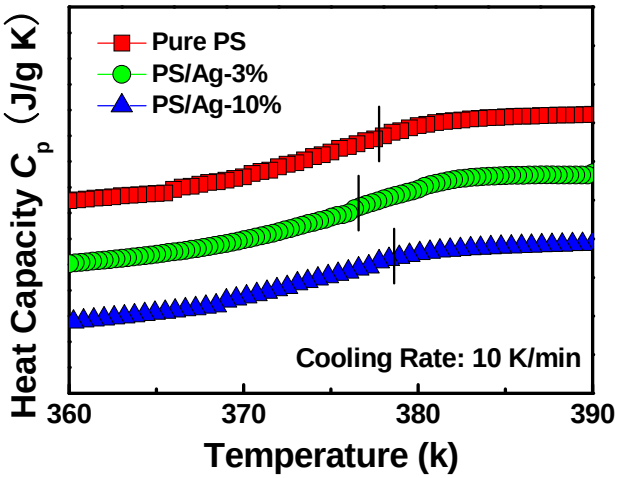

Fig. 7 DSC curves of pure PS and its nanocomposites at the cooling rate of 10 K/min. The solid lines show the position of T_g.

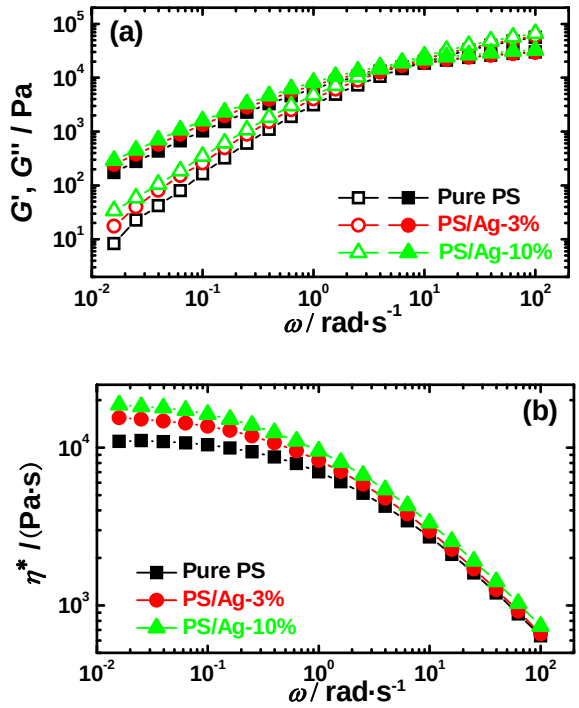

Fig. 8 Frequency dependences of (a) dynamic storage modulus (open symbols) and loss modulus (filled symbols) and (b) complex viscosity for pure PS and PS/Ag nanocomposites at 473 K.

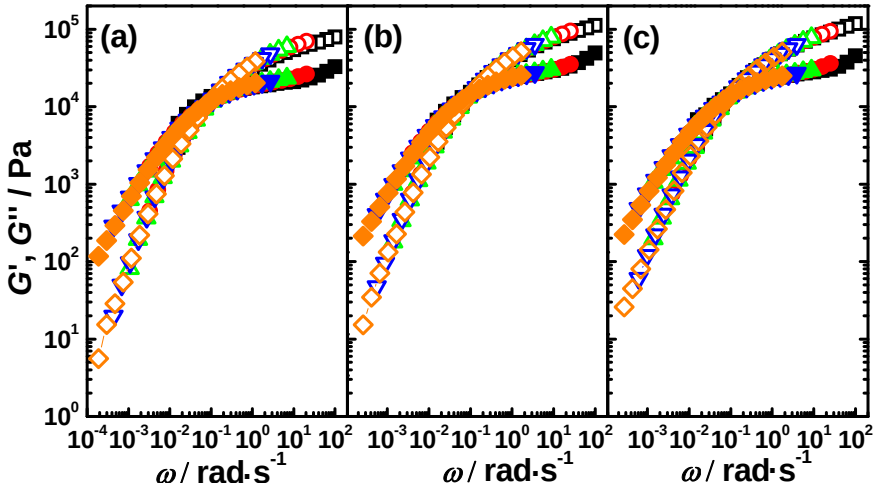

Fig. 9 Master curves of dynamic storage modulus (open symbols) and loss modulus (filled symbols) for (a) pure PS, (b) PS/Ag-3% and (c) PS/Ag-10% nanocomposites at the reference temperature of 433 K. (□, ■) 433 K, (○, ●) 443 K, (△, ▲) 453 K, (▽, ▼) 463 K and (◇, ◆) 473 K.

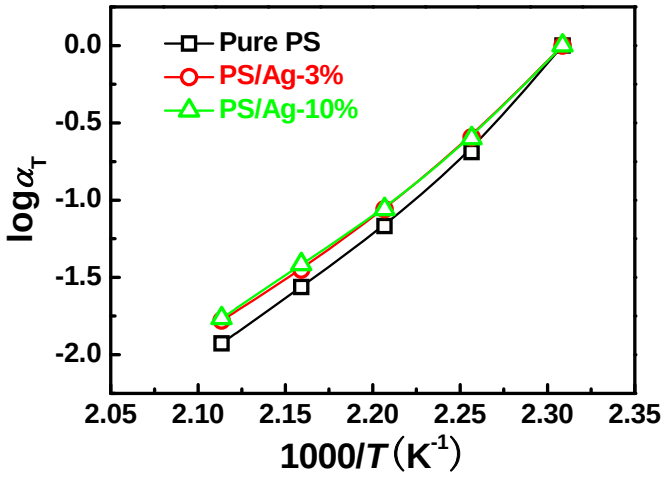

Fig. 10 Temperature dependences of horizontal shift factors for pure PS and PS/Ag nanocomposites at the reference temperature of 433 K.

Segmental dynamics and physical aging of polystyrene/silver nanocomposites

Yu Lin,[ab] Langping Liu,[b] Jiaqi Cheng,[a] Yonggang Shangguan,[*a] Wenwen Yu,[a] Biwei Qiu,[a] and Qiang Zheng,[*a]

We report the complicated variation trend of calorimetric T_g and physical aging in PS/Ag nanocomposites, despite the invariant segmental dynamics with increasing silver nanoparticle loading.

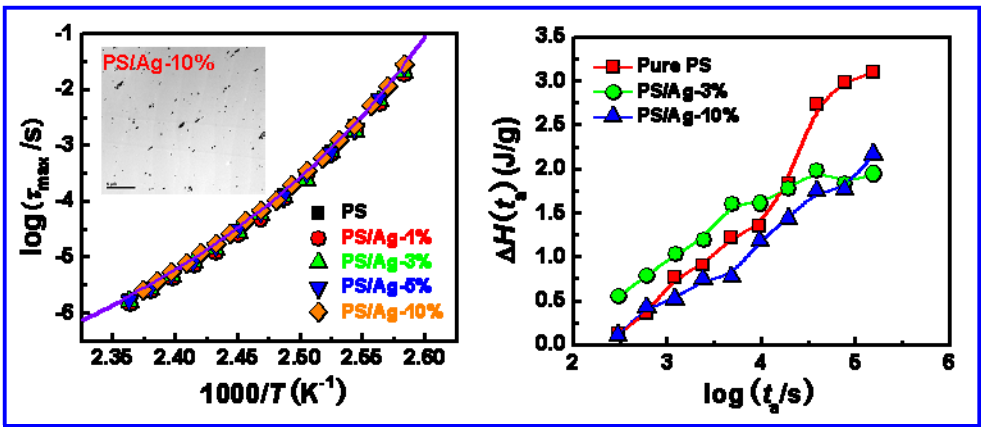

[*]Corresponding authors. Tel./fax: +86 571 8795 2522.
E-mail addresses: shangguan@zju.edu.cn (YG. Shangguan), zhengqiang@zju.edu.cn (Q. Zheng).